



LAWRENCE
LIVERMORE
NATIONAL
LABORATORY

On the Possibility of the Sheath-Driven, Finite-Beta Modes Localized Near the Divertor Plate

R.H. Cohen, D.D. Ryutov

February 10, 2005

Plasma Physics & Controlled Fusion

Disclaimer

This document was prepared as an account of work sponsored by an agency of the United States Government. Neither the United States Government nor the University of California nor any of their employees, makes any warranty, express or implied, or assumes any legal liability or responsibility for the accuracy, completeness, or usefulness of any information, apparatus, product, or process disclosed, or represents that its use would not infringe privately owned rights. Reference herein to any specific commercial product, process, or service by trade name, trademark, manufacturer, or otherwise, does not necessarily constitute or imply its endorsement, recommendation, or favoring by the United States Government or the University of California. The views and opinions of authors expressed herein do not necessarily state or reflect those of the United States Government or the University of California, and shall not be used for advertising or product endorsement purposes.

On the possibility of the sheath-driven, finite-beta modes localized near the divertor plate

R.H. Cohen, D.D. Ryutov

Lawrence Livermore National Laboratory, Livermore, CA 94551

Abstract

It is shown that, in a finite beta plasma, there may exist sheath driven modes whose amplitude decreases exponentially with the distance from the divertor plate. The modes are sensitive to the radial tilt of the divertor plate. The short-wavelength branch of the instability, with the cross-field wavelength λ_D of order of a few ion gyroradii, is present in the case of a “positive” tilt of the divertor plate, whereas the long-wavelength branch, with λ_D of order of 10 or so gyroradii is unstable for the opposite sign of the tilt. The parallel e-folding length becomes less than the distance from the plate to the X point (thereby making the mode insensitive to the processes near the X-point and the upper scrape-off layer) at the plasma betas exceeding $(2-3) \cdot 10^{-4}$. A detailed analysis of the dispersion relations is provided. The features of the modes that can be used for their experimental identification are discussed. It is pointed out that the analog of these modes may also exist in linear plasma devices with shaped end electrodes.

I. INTRODUCTION

A magnetized plasma, whose length along the field lines is limited by conducting end plates, often experiences very strong instabilities driven by a combination of two factors: cross-field variation of plasma parameters, and sheath boundary conditions at the plates.

A first rough assessment of the aforementioned fast instability was made in 1965 by Kadomtsev [1]. More recently, it was realized that such instabilities may play a role in fusion devices and analyses accounting for a variety of factors existing in such devices were made: In Ref. [2], it was emphasized that, among the driving factors, the most significant is the gradient of the electron temperature; effects of a finite beta were also taken into account. In Ref. [3], in the case of a zero-beta plasma, the role of finite Larmor radius effects was quantitatively accounted for. In Ref. [4] the instability was generalized to include resistive effects, together with electron inertia effects. In Ref. [5] the effect of a tilt of the end plate with respect to the magnetic field was included and was found to have a significant effect on the growth rate. In Ref. [6] effect of collisions with neutrals was considered. In Ref. [7] the interference between Kelvin-Helmholtz modes and the sheath-driven instability was analyzed and the conclusion was drawn that, at short wavelengths, the sheath-driven instability is dominant, and in Ref. [8] these results were confirmed by numerical simulations.

In all these papers, the instability was analyzed for a slab geometry and a uniform magnetic field. In Ref. [9], it was noted that there is a difficulty in applying the results of these studies to a tokamak with divertor, because extremely strong shearing of the flux tube in the X-point area makes irrelevant the flute model used in these earlier studies. A possible approach to a solution of this problem was offered in Ref. [10] where it was suggested that, for long-enough divertor legs, one can account for the X-point effect by imposing a boundary condition at some “control plane” situated somewhat below the X point. The boundary condition is of a resistive nature, relating the tangential current to the tangential electric field, with the electrical conductivity $\sigma = \omega_{pe}^2 / 4\pi\omega_{ce}$ (here ω_{pe} and ω_{ce} are the electron plasma and the electron cyclotron frequency, respectively). With this boundary

condition imposed, the sheath driven instability is re-established; it is now present only in the divertor leg, between the divertor plate and the control surface, with some minor, very small-scale perturbations reaching the zone slightly above the X point. {We note that the X-point effects have a strong influence also on modes localized in the main part of the scrape-off-layer and lead to the appearance of so-called “resistive x-point modes” [11,12].}

The divertor-leg instability found in Ref. [10] is very strong, with a growth time $\tau \equiv 1/\text{Im}\omega$ being typically much shorter than the plasma transit time through the divertor leg, L/v_{ti} , where L is a connection length between the divertor plate and the X point. It may even become shorter than the Alfvén transit time L/v_A . In such a case, one can expect the formation of modes which would be localized near the divertor plate, exponentially decreasing along the field line as $\exp(-s/v_A \tau)$, where s is a distance along a field line. If the growth time is short enough,

$$\tau < L/v_A, \quad (1)$$

the mode becomes localized near the divertor plate and becomes completely detached from the X point region.

Clearly, as the presence of this mode is related to the perturbation of the magnetic field, this is a finite-beta mode. An attempt to find such modes was made in an early paper [3], but the conclusion was drawn that they do not exist. In Ref. [13], an evanescent mode was found in the case of a strong-enough parallel velocity shear, i.e. the $E \times B$ velocity varying along the field line. [The origin of this shear is related to the possible variation of the electron temperature along the field lines and the resulting variation of the electrostatic potential.]

In this article, we revisit the problem of the evanescent modes in a setting similar to that of Ref. [2], i.e., without a parallel velocity shear, but with an important new element added: the non-normal intersection of the magnetic field with the divertor plate (in Ref. [2], only the case of normal intersection was considered). As we show, in the presence of the tilt, evanescent modes become possible at a finite plasma beta, and their growth rate can become quite high for a strong tilt. Interestingly, the direction of the radial tilt of the plate affects the sign of $\text{Im}\omega$, making the modes that are stable for one direction of the tilt, unstable for the opposite sign of the tilt. This effect could be used as an identifier of the modes.

Instabilities considered in Ref. [1-10, 13] exist even at zero magnetic-field-line curvature and are in this respect very different from the curvature-driven flute and ballooning modes. As was demonstrated in 1965 by Kunkel and Guillory [14], sheath boundary conditions can have strong influence on these modes, too, by removing the line-tying constraint on the conducting end surface. The analyses of the corresponding instabilities were presented by Nedospasov [15] and Garbet et al [16]. We do not include the curvature effects in this paper; the growth rate that we find is very large even for straight field lines.

This paper deals only with a linear analysis of the modes. Potentially, these modes may serve as a seed for various nonlinear structures, e.g., blobs [17], which would be in this case localized in the divertor legs, but we do not go into this issue, leaving nonlinear effects for further studies. [Note that the blobs considered in [17] were driven by curvature effects.] Here we concentrate on a linear problem in the simplest setting (as even this case turns out to be rather complex). On the other hand, we analyze in some detail how our modes behave not only in tokamaks but also in linear plasma devices such as LAPD [18]. It turns out that the finite-beta modes exist in such devices as well, and conditions for their experimental study may be more easily achieved than in divertors of large tokamaks.

The structure of this paper is as follows: In Sec. II we describe the geometry of the problem and characterize the main assumptions. In Sec. III we consider perturbations in the bulk plasma where they are shear Alfvén waves. We derive an expression for the perturbed current normal to the sheath (and the divertor plate). In Sec. IV, we derive an expression for the same current based on the sheath boundary condition. In Sec. V, by equating the two expressions, we obtain the general dispersion relation and then analyze it for various

particular cases. In Sec. VI we modify our analysis in order to cover the same instability in linear devices with shaped end electrodes. In Sec. VII we discuss experimental signatures of the instability, in particular, its characteristic frequencies, as well as relations between perturbations of various quantities. Finally, Sec. VIII contains a brief discussion of our results.

II. MAIN ASSUMPTIONS

We consider the slab geometry shown in Fig. 1. The axes x , y , and z are the analogs of the radial, poloidal, and toroidal directions. As was shown in Refs. [2,3], the main drive for the instability is related to the electron temperature gradient. Accordingly, to visualize the instability in the most clear way, we assume that the unperturbed electron temperature is a function only of radius, $T_e = T_e(x)$, while the unperturbed density and ion temperature are assumed to be uniform both in the radial and poloidal directions. We denote the (radial) length-scale of the unperturbed electron temperature variation as Δ :

$$\Delta \equiv \left| \frac{T_e'}{T_e} \right|^{-1} \quad (2)$$

where the prime means the derivative with respect to x .

The magnetic field in Fig. 1 points into the divertor plate and is such that $B_z > 0$, $B_y < 0$. Instead of B_y and B_z , we will often use the notation

$$B_T \equiv B_z > 0; \quad B_P \equiv -B_y > 0, \quad (3)$$

with the subscripts “ T ” and “ P ” referring to the toroidal and poloidal fields, respectively.

A very important feature of the problem is the presence of the “radial tilt” of the divertor plate, which is characterized by the angle α . As we will see shortly, the instability depends on the mutual orientation of the temperature gradient and the normal to the divertor plate which can be characterized by the quantity $\text{sign}(-\mathbf{n} \cdot \nabla T_e) = \text{sign}(-T_e') \tan \alpha$. For the orientation of the coordinate axes considered in this paper (Fig. 1), this quantity is positive if T_e decreases along x , and α is positive. We call this case “positive tilt”.

We consider a low recycling case, where all the plasma approaching the divertor plate is absorbed by it, and the incoming plasma is not perturbed by the neutrals formed at the plate. The plasma streams towards the divertor plate with a parallel velocity u ; we assume that it exceeds the sound speed. We assume that the unperturbed current to the plate is zero, and that the plate potential is zero.

Under such circumstances, the unperturbed plasma potential just outside the sheath is

$$\varphi_0(x) = \frac{T_e(x)}{e} \Lambda, \quad (4)$$

where $\Lambda=2-4$ is a logarithmic factor weakly depending on the plasma parameters. This sheath potential drop, in the case of a tilted magnetic field, occurs in two steps: part of the potential drop occurs in the ion sub-sheath, on a scale of order of the ion gyroradius, and the rest occurs in the Debye sheath near the wall [19]. Aside from this variation across the sheath, the unperturbed potential does not vary along a field line.

The unperturbed electric field $E_{0x} = -d\varphi_0/dx \approx -(\Lambda/e)dT_e/dx$ creates a cross-field plasma flow perpendicular to the magnetic field

$$\mathbf{v}_{Dy} = -c \frac{E_x B_z}{B^2}, \quad \mathbf{v}_{Dz} = c \frac{E_x B_y}{B^2}, \quad (5)$$

which also does not vary along field lines. We assume that the poloidal projection of the drift velocity is less than the poloidal projection of the parallel flow velocity u , i.e.,

$$v_D < u \frac{B_T}{B_P} \quad (6)$$

In the opposite case, there may (formally) occur a reversal of the poloidal flow; even the equilibrium state for this situation is not fully understood and we do not attempt to cover it in this paper. The condition (6) can also be formulated as:

$$\frac{\rho_i}{\Delta} < \frac{B_P}{B_T}, \quad (7)$$

where ρ_i is the ion gyro-radius evaluated for the electron temperature:

$$\rho_i \equiv \frac{m_i}{eB} \sqrt{\frac{2T_e}{m_i}} \quad (8)$$

If the distance between the divertor plate and the X point along the field lines is L , then the distance projected along the y direction is, obviously,

$$l = \frac{LB_P}{B} \quad (9)$$

The parameter l represents the length of the divertor leg. We assume that l is much greater than the thickness Δ of the scrape-off layer. This is a “long-leg” approximation, which justifies the assumption that the magnetic field can be considered as uniform, at least not very far from the divertor plate.

III. PERTURBATIONS IN THE BULK PLASMA

The physical mechanism of the instability at a negligible plasma beta can be addressed in the model of moving flux tubes. If a flux tube, with the plasma occupying it, is displaced in the radial direction, its potential with respect to the conducting plate remains the same as before displacement (because this potential is determined by T_e , which is convected together with the flux tube). On the other hand, the ambient plasma, which has a different temperature, has a different potential. Therefore, a cross- \mathbf{B} electric field emerges. A more detailed analysis shows that the $\mathbf{E} \times \mathbf{B}$ drift is phased in such a way that it leads to the instability.

As we have mentioned in the Introduction, the typical growth rate is quite high, much higher than the inverse transit time of the plasma from the X-point to the divertor plate. One may therefore expect that at a finite (albeit small) beta, the growth rate would exceed the inverse Alfvén transit time. In such a case, the perturbation loses its flute nature and becomes a shear-Alfvén mode instead. A localized unstable mode can be formed near the divertor plate if the condition (1) holds.

We seek perturbations with temporal dependence $\sim \exp(-i\omega t)$. We assume that the radial length-scale of perturbations is small compared to the thickness Δ . This allows use of an eikonal approximation in the x direction and seeking x -dependence in the form of $\exp(ik_x x)$. The “toroidal” direction (z) is an ignorable coordinate; hence the dependence on it can be taken as $\exp(ik_z z)$. There is no dependence of the plasma parameters on the coordinate y , either, so, the y -dependence can be sought in the form $\exp(iK_y y)$, where K_y is some constant, which is complex for the localized modes. It is convenient to present K_y in the form: $K_y = q + k_y$, with k_y satisfying the equation $k_y = -k_z B_z / B_y$ (which means that vector \mathbf{k} is perpendicular to the magnetic field). With Eq. (3) taken into account, the condition $k_y = -k_z B_z / B_y$ can be written as

$$B_P k_y = B_T k_z \quad (10)$$

In other words, we are seeking a solution of the form:

$$\exp(i\mathbf{K} \cdot \mathbf{r}) \equiv \exp(iqy) \exp(i\mathbf{k} \cdot \mathbf{r}) \quad (11)$$

with

$$K_x = k_x, K_y = q + k_y, K_z = k_z \quad (12)$$

and the vector \mathbf{k} satisfying condition (10). The convenience of this representation is in that the second multiplier in the r.h.s. of Eq. (11) does not vary along the field line and describes a pure flute perturbation, whereas the first multiplier describes a slow variation of perturbations along the field line. One obviously has:

$$\mathbf{B} \cdot \nabla [\exp(i\mathbf{K} \cdot \mathbf{r})] = -iqB_p \exp(i\mathbf{K} \cdot \mathbf{r}) \quad (13)$$

For the further analysis, it is convenient to introduce the displacement vector ξ which is defined by the equation:

$$\frac{d\xi}{dt} = \delta\mathbf{v}, \quad \frac{d}{dt} \equiv -i\omega + \mathbf{v}_0 \cdot \nabla, \quad (14)$$

where $\delta\mathbf{v}$ is the velocity perturbation and \mathbf{v}_0 is the unperturbed velocity, which has components perpendicular to the magnetic field (Eq. (5)) and parallel to the magnetic field (the parallel flow velocity u). For perturbations of the form (11), one has:

$$\frac{d}{dt} = -i\omega + i\mathbf{k} \cdot \mathbf{v}_D + iq \frac{v_D B_T + u B_p}{B} \quad (15)$$

According to Eq. (6), one can neglect the term $v_D B_T$ compared to $u B_p$ in Eq. (15).

The qualitative picture presented in the introduction and at the beginning of this section shows that the perturbation varies along the field line on the scale v_A/ω . In other words, q in Eq. (15) can be estimated as $(\omega/v_A)(B/B_p)$. Therefore, the term proportional to u in Eq. (15) contains a small parameter $(u/v_A) \sim (\beta)^{1/2} \ll 1$ compared to the first term in the right hand side of Eq. (15). Therefore, we conclude that, to a high accuracy (the parameter β for the tokamak divertors lies usually between $3 \cdot 10^{-5}$ and 10^{-3}),

$$\delta\mathbf{v} = -i\Omega\xi \quad (16)$$

with

$$\Omega \equiv \omega - \mathbf{k} \cdot \mathbf{v}_D \quad (17)$$

The linearized momentum equation, the line-tying equation, and the Biot-Savars' law can then be written as:

$$-\Omega^2 m_i n \xi = -\nabla \delta p + \frac{\delta \mathbf{j} \times \mathbf{B}}{c} \quad (18)$$

$$\delta \mathbf{B} = \nabla \times [\xi \times \mathbf{B}] \quad (19)$$

$$\nabla \times \delta \mathbf{B} = \frac{4\pi}{c} \delta \mathbf{j} \quad (20)$$

By noting that the displacement ξ in the Alfvén wave is perpendicular to both the wave vector and the unperturbed magnetic field, one obtains from Eq. (19) that

$$\delta \mathbf{B} = iB_p q \xi \quad (19')$$

Plugging this result into Eq. (20) and taking the scalar product of Eq. (18) with the vector $\mathbf{K} \times \mathbf{B}$, one finds:

$$q = \pm \frac{\Omega}{v_A} \frac{B}{B_p} \quad (21)$$

In Eq. (21), in order to avoid the divergence of the solution at large y , one has to choose the positive sign for the unstable mode ($\text{Im}\omega = \text{Im}\Omega > 0$) and the negative sign for the stable mode ($\text{Im}\omega = \text{Im}\Omega < 0$). In the following derivation we will be concerned with the unstable mode.

One sees that the e-folding length (in y) of the perturbation is $(v_A/\text{Im}\Omega)(B_p/B)$ and, in order to have the perturbation damped before it reaches the X point, the following condition has to be satisfied: $(v_A/\text{Im}\Omega)(B_p/B) < l$, where l is defined by Eq. (9). Using Eq. (9), one can also rewrite this condition as:

$$\frac{\text{Im}\Omega L}{v_A} > 1 \quad (22)$$

This condition coincides with Eq. (1) introduced on the basis of qualitative considerations.

The pressure perturbation for incompressible modes (which includes the Alfvén mode) is determined solely by the plasma convection:

$$\delta p = -n \xi_x T'_e \quad (23)$$

Using this expression and Eq. (10), it is straightforward to obtain from the set (17)-(19) that, for perturbations of the form $\exp(i\mathbf{K} \cdot \mathbf{r})$,

$$\delta \mathbf{j}_{\parallel} = -\frac{c\Omega B_T}{4\pi v_A k_y} \left(k_x^2 + k_y^2 \frac{B^2}{B_T^2} \right) \frac{\mathbf{B}}{B} \xi_x = -\frac{c\Omega B_T k^2}{4\pi v_A k_y} \frac{\mathbf{B}}{B} \xi_x \quad (24)$$

$$\delta \mathbf{j}_{\perp} = \frac{c\Omega B_T}{B^2 k_y} \left(-\Omega m_i n \mathbf{k} + \frac{i n T'_e k_y}{\Omega B_T} \mathbf{k} \times \mathbf{B} \right) \xi_x \quad (25)$$

Wherever possible, we have used the smallness of the parameter q/k_y .

We can now find the normal component of the current in terms of the plasma displacement on the plasma side of the sheath,

$$\mathbf{n} \cdot \delta \mathbf{j} = \mathbf{n} \cdot \delta \mathbf{j}_{\parallel} + \mathbf{n} \cdot \delta \mathbf{j}_{\perp} = \xi_x \left[\frac{c k^2 \Omega}{4\pi v_A k_y} \frac{B_p B_T}{B} \cos \alpha + i \frac{c n B_T T'_e}{B^2} \left(k_y \frac{B^2}{B_T^2} \sin \alpha - k_x \cos \alpha \right) \right] \quad (26)$$

We have neglected the contribution of the first term in the brackets in Eq. (25) because it contains a small parameter $\sim \Omega/kv_A$ compared to the contribution from $\mathbf{n} \cdot \delta \mathbf{j}_{\perp}$.

IV. THE SHEATH BOUNDARY CONDITION

IV. A Perturbations near the divertor plate: curl-free electric field

The divertor plate is a perfect conductor, so that the tangential component of the electric field at that surface is zero. At a distance of a few ion gyro-radii, where we impose the boundary conditions, the electric field can be considered as curl-free. Indeed, the vortex component of the electric field that can be evaluated from equation $\nabla \times \delta \mathbf{E}_{\text{vortex}} = -\omega \delta \mathbf{B}/c$, is of order of $\delta E_{\text{vortex}} \sim (\omega/c k) \delta B \sim \omega B \Omega \xi_x / v_A c k$ (see Eqs. (19') and (21)) whereas the potential component is $\delta E_{\text{pot}} \sim \xi_x \Omega B / c \gg \delta E_{\text{vortex}}$ (see Eq. (29) below). The presence of the potential electric field at the plasma side of the sheath allows the flux tube to slide over the surface, despite the fact that the magnetic field perturbation is almost zero. This is how the line-tying condition breaks down in the presence of sheaths – an observation made by Kunkel and Guillory in 1965.

What we basically say, is that the magnetic field perturbation near the wall is negligible; therefore, there is no paradox associated with the condition that the normal

component of the magnetic field cannot be perturbed. In our case even *the total* perturbation is negligibly small. The magnetic field perturbations play a role only at the scale $\sim v_A/\Omega$.

Based on these considerations, we can present $\delta\mathbf{E}$ in the vicinity of the plate as

$$\mathbf{E} = -\nabla\delta\varphi \quad (27)$$

This means that, near the divertor plate,

$$\boldsymbol{\xi} = \frac{c\delta\varphi}{\Omega B^2} \mathbf{K} \times \mathbf{B} \quad (28)$$

and, in particular,

$$\xi_x = \frac{ck_y\delta\varphi}{\Omega B_T} \quad (29)$$

Here we have taken into account Eq. (10).

IV. B Relating the current perturbation and the plasma displacement

In this section we will find the normal projection of the current perturbation on the divertor plate, based on the current-voltage characteristic derived in the earlier papers [20, 21]. To be more precise, we have to find the current on the plasma side of the sheath, as the currents on the plate and on the plasma side of the sheath, generally speaking, are different [20].

The required current-voltage characteristic, prior to the linearization, has the form [20]:

$$\mathbf{n} \cdot \mathbf{j} = -en \frac{B_p}{B} \cos\alpha \left[u - v_{Te} \exp\left(-\frac{e\varphi}{T_e}\right) \right] + env_{Dx} \sin\alpha + env_{Dy} \cos\alpha \quad (30)$$

where \mathbf{v}_D is the velocity of the $\mathbf{E} \times \mathbf{B}$ drift (5). The plate is assumed to be conducting and at the zero potential. In the unperturbed state, the current to the wall is assumed to be zero:

$$\mathbf{n} \cdot \mathbf{j}_0 = 0. \quad (31)$$

The quantities that experience perturbation are the electron temperature, the drift velocity and, generally speaking, the parallel flow velocity and the tangential component of the magnetic field. We will, however, ignore the latter two because their contribution is small. Perturbing Eq. (30) and taking into account these comments, one readily finds:

$$\begin{aligned} \mathbf{n} \cdot \delta\mathbf{j} = & -en \frac{B_p}{B} \cos\alpha \left(u - \frac{B}{B_p} v_{0Dy} \right) \left[(\Lambda + 0.5) \frac{\delta T_e}{T_e} - \frac{e\delta\varphi}{T_e} \right] \\ & + en\delta v_{Dx} \sin\alpha + en\delta v_{Dy} \cos\alpha \end{aligned} \quad (32)$$

The second term in the round brackets can be ignored because of inequality (6). Using also Eq. (29) and equation $\delta T_e = -\xi_x T_e'$, one can express the r.h.s. of Eq. (32) in terms of the x -component of the plasma displacement near the surface of the divertor plate:

$$\mathbf{n} \cdot \delta\mathbf{j} = -en\xi_x \left\{ u \frac{B_p}{B} \cos\alpha \left[(\Lambda + 0.5) \frac{T_e'}{T_e} + \frac{e\Omega B_T}{cT_e k_y} \right] + i \frac{\Omega}{k_y} \left(k_y \sin\alpha - k_x \frac{B_T^2}{B^2} \cos\alpha \right) \right\} \quad (33)$$

Eq. (33) coincides, up to notation, with the boundary condition of Ref. [21].

V. DISPERSION RELATION AND ITS ANALYSIS

V.A General dispersion relation

Equating two expressions for the normal component of the current – the one obtained from the solution for the mode in the bulk plasma (Eq. (26)), and the other obtained from the sheath boundary condition (Eq. (33)), one arrives at the following dispersion relation:

$$\frac{\Omega}{v_A} \left[1 + \frac{2\sqrt{\beta_e} u}{k^2 \rho_i^2 v_i} - i \frac{B^2 \sqrt{\beta_e}}{B_p B_T k \rho_i} \left(-\frac{k_y}{k} \tan \alpha + \frac{k_x B_T^2}{k B^2} \right) \right] = \frac{T_e' \beta_e}{T_e} \left[i \frac{B^3}{2B_p B_T^2} \frac{k_y}{k} \left(-\frac{k_y}{k} \tan \alpha + \frac{k_x B_T^2}{k B^2} \right) - \frac{k_y}{k^2 \rho_i v_i} \frac{B}{B_T} (\Lambda + 0.5) \right] \quad (34)$$

where

$$v_i = \sqrt{\frac{2T_e'}{m_i}}; \quad \rho_i = \frac{v_i}{\omega_{Ci}}; \quad \omega_{Ci} = \frac{eB}{m_i c}; \quad \beta_e = \frac{8\pi n T_e'}{B^2}, \quad (35)$$

and m_i is the ion mass. We see that the instability can be present only for the non-zero temperature gradient and disappears if $T_e' = 0$ (when Ω becomes zero).

As the mode is assumed to be localized near the divertor plate, the distance L to the X point does not enter Eq. (34). However, as the very possibility of the existence of the localized mode requires fulfillment of the condition (22), we sometimes present Ω in the units of v_A/L . The mode exists as a localized mode if $\text{Im } \Omega L/v_A > 1$. An expression for the growth rate that can be easily obtained from Eq. (34) is:

$$\text{Im } \frac{\Omega L}{v_A} = \frac{T_e' L \beta_e}{T_e} \frac{B^3}{2B_p B_T^2} \frac{k_y \rho_i \left(-k_y \rho_i \tan \alpha + k_x \rho_i \frac{B_T^2}{B^2} \right) \left[k^2 \rho_i^2 - \frac{B_T^2}{B^2} \frac{u}{v_i} \sqrt{\beta_e} (2\Lambda - 1) \right]}{\left(k^2 \rho_i^2 + \frac{2\sqrt{\beta_e} u}{v_i} \right)^2 + \beta_e \left(\frac{B^2}{B_p B_T} \right)^2 \left(-k_y \rho_i \tan \alpha + k_x \rho_i \frac{B_T^2}{B^2} \right)^2} \quad (36)$$

V.B An instability at a significant tilt

At a substantial tilt of the divertor plate, $|\tan \alpha| > 1$, the terms of the form $k_x \rho_i B_T^2 / B^2$ in Eq. (36) can be neglected. Then, as the denominator in (36) contains a higher (the fourth) power of k compared to the numerator, the instability has the highest growth rate if we make k_x much less than k_y , so that $k^2 = k_y^2 B^2 / B_T^2$ (see Eq. (10)). This is the ordering used also in the earlier papers [5, 10]. (Later on, in Sec. V.E, we return to this issue again, for a more detailed analysis: the k_x terms are important in the zero-tilt case.)

In the approximation $k_y > k_x$, one obtains from (34) the following simplified dispersion relation:

$$\frac{\Omega L}{v_A} \left[1 + \frac{2B_T^2 \sqrt{\beta_e} u}{B^2 k_y^2 \rho_i^2 v_i} + i \frac{B_T \sqrt{\beta_e}}{B_p k_y \rho_i} \tan \alpha \right] = -\frac{T_e' L \beta_e}{T_e} \left[i \frac{B}{2B_p} \tan \alpha + \frac{B_T}{B k_y \rho_i v_i} u (\Lambda + 0.5) \right] \quad (37)$$

In order to establish connection of this result with the earlier studies of the effect of the tilt [5,10], we rewrite this equation using the same notation as in these earlier papers:

$$\Omega_{V_A} + \frac{B_T^2}{B^2} \Omega \Omega_1 L + i \frac{B_T}{B} \Omega \Omega_2 L + \Gamma_1^2 L + i \Gamma_2^2 L = 0, \quad (38)$$

where

$$\Omega_1 = \frac{\omega_{Ci}^2 M u}{L k_y^2 T_e}; \quad \Omega_2 = \frac{\omega_{Ci}}{k_y l} \tan \alpha; \quad \Gamma_1^2 = \left(\Lambda + \frac{1}{2} \right) \frac{\omega_{Ci} u T_e'}{k_y L T_e}; \quad \Gamma_2^2 = \frac{T_e'}{M l} \tan \alpha \quad (39)$$

and l is introduced by Eq. (9).

By tracing the origin of various terms in Eq. (39) to the basic equations of Sections III and V, one can identify the meaning of these terms: The first term in the l.h.s. represents the inertia of the plasma occupying the wiggling flux tube; the second term describes the sheath resistance as discussed by Kunkel and Guillory [14]; the third term describes an effect of the tilt on the sheath CVC as first described in Ref. [5]; the fourth term first introduced by Kadomtsev [1] describes reaction of the sheath potential on the change of the temperature caused by the motion of the foot point of the flux tube over the surface; the fifth term describes the role of the pdV work performed by the advancing (recessing) boundary in the frame attached to the flux tube foot-point [21]. Note that the connection length L actually drops from Eq. (38), as the characteristic frequencies introduced by Eq. (39) also depend on L . [There is a typo in the expression for Γ_2 in Ref. 10, where L instead of l is written in the denominator; this typo does not, however, propagate to the further equations; note also that in Ref. [10] the definition of α differs from the definition of our present paper by $\pi/2$.]

The main difference from the dispersion relation of Ref. [5] is in the form of the very first (inertial) term, which was equal to $\Omega^2 L$ in the case of a zero-beta plasma limited from both sides, with L being the distance between two plates limiting the plasma. The other difference is that we now do not make an assumption that B_p is small compared to B_T , thereby including the parameter domain characteristic of spherical tokamaks. This is reflected by the presence of the factor (B_T/B) in Eq. (38).

An expression for the instability growth rate can be easily obtained from Eq. (37):

$$\frac{\text{Im} \Omega L}{v_A} = - \frac{T_e' L \beta_e}{2 T_e} \frac{B}{B_p} \tan \alpha \frac{k^2 \rho_i^2 \left[k^2 \rho_i^2 - \frac{B_T^2}{B^2} \frac{u}{v_i} \sqrt{\beta_e} (2\Lambda - 1) \right]}{\left(k^2 \rho_i^2 + \frac{2 B_T^2}{B^2} \frac{u}{v_i} \sqrt{\beta_e} \right)^2 + \beta_e k^2 \rho_i^2 \left(\frac{B}{B_p} \tan \alpha \right)^2}, \quad (40)$$

Before switching to its general analysis, we present some results for the case of some “generic” divertor of a mid-size tokamak, where

$$\frac{B}{B_p} = 5, \quad \frac{B}{B_T} \approx 1, \quad \frac{L |T_e'|}{T_e} = 300, \quad \beta_e = 10^{-3}, \quad \frac{u}{v_i} = 1.5 \quad (41)$$

Fig. 2 shows the dependence of the growth rate vs. the wave number, for several values of the tilt, for $\Lambda=2$. As we see, two modes of oscillations can be distinguished: the short-wavelength mode, and a long-wavelength mode. The transition between the two modes occurs at the point where the growth rate is zero, i.e., at

$$k_y^{(crit)} \rho_i = \frac{B_T}{B} \left[\frac{u^2 (2\Lambda - 1)^2 \beta_e}{v_i^2} \right]^{1/4} \quad (42)$$

For a given sign of the temperature gradient, the stability or instability of each branch depends on the sign of the tilt. In a common flux region, where $T_e' < 0$, the short-wavelength mode is unstable at a positive tilt of the plate, $\alpha > 0$, whereas the long-wavelength mode is unstable at a negative tilt, $\alpha < 0$. In the private flux region, the situation is opposite.

V.C The short-wavelength mode

When considering the short-wavelength mode, one should remember that, because of the approximations made in our general equations, we cannot increase k_\perp beyond the inverse ion gyro-radius. The maximum growth rate is reached at the boundary of the applicability domain. For not very strong tilts, this growth rate can be approximated as

$$\max \left(\text{Im} \frac{\Omega^{(s)} L}{v_A} \right) = - \frac{T_e' L \beta_e}{2 T_e} \frac{B}{B_p} \tan \alpha \quad (43)$$

where “s” stands for “short”. This mode will be localized below the X point if the condition (22) holds, i.e., if

$$\beta_e > \frac{2 T_e}{T_e' L} \frac{B_p}{B \tan \alpha} \quad (44)$$

For the set of parameters as in Eq. (41), and $\tan \alpha = 5$, the localized mode can exist at $\beta_e > 2.5 \cdot 10^{-4}$.

For the short wavelength modes it may be necessary to use a more general dispersion relation for Alfvén waves, $\Omega^2 = v_A^2 k_\parallel^2 / (1 + \omega_{pe}^2 k_\perp^2 / c^2)$ [4], instead of simply $\Omega^2 = v_A^2 k_\parallel^2$, as we did in this paper. The applicability condition for our approach is that $\omega_{pe}^2 k_\perp^2 / c^2 < 1$. For the shortest wavelengths considered above, $k_\perp \sim \rho_i$, this condition reduces to $\beta_e > m_e / m_i$. For the critical wave number (42), i.e., at the transition from short to long wavelength mode, the condition $\omega_{pe}^2 k_\perp^2 / c^2 < 1$ reduces to

$$\beta_e > \left(\frac{m_e}{m_i} \right)^2 \left[\frac{u}{v_i} (2\Lambda - 1) \right]^2 \quad (45)$$

and holds by a substantial margin in all realistic situations.

V.D The long-wavelength mode

To study this mode, it is convenient to present the frequency and the wave number in the normalized form,

$$\Omega = \tilde{\Omega} \Omega_0, \quad k = \tilde{k} k_0 \quad (47)$$

with the normalization parameters being

$$\Omega_0 = v_A \beta_e^{3/4} \left| \frac{T_e'}{T_e} \right| \frac{B_T}{B} \sqrt{\frac{u}{2 v_i}} \quad (48)$$

and

$$k_0 = \frac{B_T \beta_e^{1/4}}{B \rho_i} \sqrt{\frac{2u}{v_i}} \quad (49)$$

When expressed in this way, Eq. (40) acquires a universal form, where the result depends of only one constant, C :

$$\text{Im}\tilde{\Omega} = \text{sign}(T'_e)g(C, \tilde{k}); \quad g(C, \tilde{k}) \equiv \frac{C\tilde{k}^2 \left[\Lambda - \frac{1}{2} - \tilde{k}^2 \right]}{(\tilde{k}^2 + 1)^2 + \tilde{k}^2 C^2} \quad (50)$$

where

$$C = \frac{B^2 \beta_e^{1/4}}{B_T B_p} \sqrt{\frac{v_i}{2u}} \tan \alpha \quad (51)$$

The dependence of the growth rate on various external parameters is encapsulated in a single dimensionless parameter C (the Λ does not vary much; still, the scan over Λ is presented at the end of this section). We assume that the sign of the temperature gradient is positive, so that an instability is present at positive C (positive $\tan \alpha$).

We evaluate now the maximum growth rate of the long-wavelength mode. For a given k and any given set of the system parameters, the r.h.s. of Eq. (49) has a maximum at some value of $\tan \alpha$, in other words, at some C . With this value of C chosen, the dependence (49) on k also has a maximum. Finding this maximum would yield a maximum possible growth rate as a function of $\tan \alpha$ and k . This will be just a number, $\mu \equiv \max_{C, \tilde{k}} g(C, \tilde{k})$. The corresponding analysis is presented in Appendix 1. The resulting plot of the optimum values of C_{opt} and \tilde{k}_{opt} , as well as μ vs. the parameter Λ is shown on Fig. 3. For $\Lambda = 3$, one has: $C_{opt} = 2.1$, $\tilde{k}_{opt} = 0.47$, $\mu = 0.47$. This means that the maximum growth rate for $\Lambda = 3$ is (see Eq. (47)):

$$\frac{\text{Im}\Omega L}{v_A} \approx 0.4 \beta_e^{3/4} \frac{B_T}{B} \left| \frac{T'_e}{T_e} \right| L \quad (51)$$

(we assumed $u = 1.5v_i$). It corresponds to the following wave number and $\tan \alpha$:

$$(k\rho_i)_{opt} \approx 0.8 \frac{B_T \beta_e^{1/4}}{B}, \quad (\tan \alpha)_{opt} \approx 3.8 \frac{B_T B_p}{B^2 \beta_e^{1/4}}. \quad (52)$$

According to Eq. (22), this mode will exist as a localized mode if the following condition holds:

$$\beta_e > 3.4 \left[\frac{T_e}{T'_e L} \frac{B}{B_T} \right]^{4/3} \quad (53)$$

For $T'_e L / T_e = 300$, and $B_p / B = 0.2$, β_e must exceed 0.16%. For this value of beta, one has $(k\rho_i)_{opt} \approx 0.16$, and $(\tan \alpha)_{opt} \approx 3.8$ ($\alpha \approx 75^\circ$).

V.E An instability at a zero tilt

When considering the case of a zero radial tilt ($\alpha = 0$), one has to retain the terms containing k_x in Eq. (34). For $\alpha = 0$, this equation reads as

$$\frac{\Omega L}{v_A} \left[1 + \frac{2\sqrt{\beta_e} u}{k^2 \rho_i^2 v_i} - i \frac{B_T \sqrt{\beta_e} k_x}{B_p k \rho_i} \right] = \frac{T_e' L \beta_e}{T_e} \left[i \frac{B}{2B_p} \frac{k_y k_x}{k^2} - \frac{k_y}{k^2 \rho_i} \frac{u}{v_i} \frac{B}{B_T} (\Lambda + 0.5) \right] \quad (54)$$

The growth rate is:

$$\frac{\text{Im} \Omega L}{v_A} = - \frac{T_e' L \beta_e}{2T_e} \frac{B}{B_p} \frac{k_x k_y \rho_i^2 \left[k^2 \rho_i^2 - \frac{u}{v_i} \sqrt{\beta_e} (2\Lambda - 1) \right]}{\left(k^2 \rho_i^2 + 2 \frac{u}{v_i} \sqrt{\beta_e} \right)^2 + \beta_e k_x^2 \rho_i^2 \left(\frac{B}{B_p} \right)^2} \quad (55)$$

In order to be localized, this mode requires a relatively high beta. What, however, is interesting with this mode, is that it exists (provided the beta is high enough) at any sign of the temperature gradient: the unstable perturbation is selected by the proper choice of the sign of the product $k_x k_y$.

For any realistic values of beta ($\sim 10^{-3}$ - 10^{-4}) and of the B/B_p ratio (< 20), the last term in the denominator of Eq. (55) can be neglected, thereby considerably simplifying the analysis. [Note that in the case of a substantial tilt, $\tan \alpha > 1$, the analogous term in Eq. (40) could not be dropped, because it contained a large additional factor $\tan^2 \alpha$.] With this term dropped, the maximum growth rate at a given k corresponds to equal values of k_x and k_y , i.e., to $|k_x| = |k_y| = k/\sqrt{2}$ and one has for this maximum:

$$\frac{\text{Im} \Omega L}{v_A} = -h \frac{T_e' L \beta_e}{4T_e} \frac{B}{B_p} \times \text{sign}(k_x k_y), \quad (56)$$

where

$$h \equiv \frac{k^2 \rho_i^2 \left[k^2 \rho_i^2 - \frac{u}{v_i} \sqrt{\beta_e} (2\Lambda - 1) \right]}{\left(k^2 \rho_i^2 + 2 \frac{u}{v_i} \sqrt{\beta_e} \right)^2}. \quad (57)$$

The plot of the dimensionless function h for various values of beta is shown on Fig. 4. One sees that, as before, there exist a short-wavelength and a long-wavelength branches, with the transition from one to another branch occurring at

$$k^{(crit)} \rho_i = \left[\frac{u^2 (2\Lambda - 1)^2 \beta_e}{v_i^2} \right]^{1/4} \quad (58)$$

What is, however, different, is that both branches are now unstable simultaneously, at any sign of T_e' ; the sign of T_e' determines the mutual sign of k_x and k_y of the unstable mode.

The maximum growth rate for the short-wavelength mode is reached at the applicability limit, $k \rho_i = 1$, where h is close to 1. The maximum growth rate of the long-wavelength mode is reached at

$$k^{(opt)} \rho_i = \sqrt{\frac{2u\sqrt{\beta_e}}{v_i} \frac{2\Lambda - 1}{2\Lambda + 3}}, \quad (59)$$

where

$$|h|_{\max} \approx \frac{(2\Lambda - 1)^2}{8(2\Lambda + 1)}. \quad (60)$$

For $\Lambda=3$, on has $|h|_{\max} \approx 0.45$. The absence of an additional large factor $\tan\alpha$ in the expression for the growth rate (compare Eqs. (40) and (55)) makes the growth rate in the case of a zero tilt smaller than in the case of a large tilt. Accordingly, in order for localized modes to be present at a zero tilt, the beta value must be higher than in the case of a strong tilt.

VI RELATION TO LINEAR PLASMAS

The instability that we have discussed in the previous section can be studied in linear devices, where one would use a shaped end electrode of the type shown on Fig. 5, where this electrode is simply a cone. In the eikonal approximation, one can consider flux tubes leaning on various elements of the end electrode and, for small-scale perturbations, consider the corresponding segment of the electrode as a flat surface whose normal is tilted at some angle α with respect to the axis. This brings us back to the geometry of Fig.1, with the only difference that there will be no toroidal magnetic field present in the linear device (we do not consider a situation where a large axial current is present).

To obtain a dispersion relation that describes this modified situation, it is convenient to replace k_y in the dispersion relation (34) by k_z , as given by Eq. (10). After that, one should take a limit $B_T \rightarrow 0$, $B_p \rightarrow B$ which leads to the appropriate dispersion relation:

$$\frac{\Omega L}{v_A} \left[1 + \frac{2\sqrt{\beta_e}}{k^2 \rho_i^2} \frac{u}{v_i} + i \frac{\sqrt{\beta_e}}{k \rho_i} \frac{k_z}{k} \tan \alpha \right] = -\frac{T_e' L \beta_e}{T_e} \left[i \frac{k_z^2}{2k^2} \tan \alpha + \frac{k_z}{k^2 \rho_i} \frac{u}{v_i} (\Lambda + 0.5) \right] \quad (61)$$

The coordinate axes in this case should be identified as follows (Fig. 4): x is directed radially, y is directed axially, and z is directed azimuthally.

At $\alpha=0$ (flat end surface, normal intersection) the Ω is purely real. This is in agreement with the conclusion made in Ref. [2] regarding the absence of localized modes in the case of the normal intersection. On the other hand, as Eq. (61) shows, at $\alpha \neq 0$ the localized modes become, in principle, possible.

At a given k , it is beneficial to increase the drive terms (the terms containing $\tan\alpha$) by increasing k_z (and decreasing k_x). Accordingly, we make the further analysis for the case $k_z > k_x$. In this case, the growth rate can be presented as

$$\frac{\text{Im}\Omega L}{v_A} = -\frac{T_e' L}{2T_e} \beta_e \tan \alpha \frac{k^2 \rho_i^2 \left[k^2 \rho_i^2 - \frac{u}{v_i} \sqrt{\beta_e} (2\Lambda - 1) \right]}{\left(k^2 \rho_i^2 + 2 \frac{u}{v_i} \sqrt{\beta_e} \right)^2 + k^2 \rho_i^2 \beta_e \tan^2 \alpha} \quad (62)$$

For small-enough betas, $\beta_e < 10^{-2}$, and at realistic values of $\tan\alpha < 10$, one can neglect the last term in the denominator, arriving at the expression

$$\frac{\text{Im}\Omega L}{v_A} = -\frac{T_e' L}{2T_e} \beta_e \tan \alpha \times h \quad (63)$$

where the dimensionless function h is determined by Eq. (57). The fastest-growing mode corresponds to the maximum possible wave-number, $k \rho_i \sim 1$:

$$\frac{\text{Im}\Omega^{(s)}L}{v_A} \approx -\frac{T'_e L}{2T_e} \beta_e \tan\alpha \quad (64)$$

If the temperature decreases in the outward direction, i.e. $T'_e < 0$, this short wavelength mode is unstable for the positive tilt (as on Fig. 4a). At wave-vectors smaller than the critical wave vector (58) this mode becomes stable, very much like in the case discussed in Sec. VI.B. At these smaller wave-numbers the instability is present for the negative tilt, for which the cone apex is oriented away from the plasma (Fig. 4b). The maximum growth rate of the long-wavelength mode is reached at the wave vector (59) and is equal to

$$\frac{\text{Im}\Omega^{(l)}L}{v_A} \approx \frac{(2\Lambda - 1)^2}{8(2\Lambda + 1)} \frac{T'_e L}{T_e} \beta_e \tan\alpha \quad (65)$$

We remind that, for the long-wavelength mode to be unstable, the tilt of the absorbing surface must be negative, as shown in Fig. 4b. Taking $\Lambda=3$, one sees that the growth rate of long-wavelength modes in a linear device is comparable to that of the short-wavelength modes.

Consider as an example the possibility of observing these modes at a LAPD device [18]. Assuming that the plasma density is 10^{12} cm^{-3} , the electron temperature is 10 eV, and the axial magnetic field is 600 G, one finds that the electron beta is $\sim 10^{-3}$. Then, for the radial length-scale (Eq. (2)) $\Delta \sim 5 \text{ cm}$, and the plasma length of 18 m, one finds that

$$\frac{\text{Im}\Omega L}{v_A} \sim \frac{L}{2\Delta} \beta_e \tan\alpha \sim 0.18 \tan\alpha. \quad (66)$$

We do not distinguish here between the long- and short-wavelength modes, as their maximum growth rates are close to each other. Equation (66) shows that the localized mode can be observed if $\tan\alpha > 5$, or equivalently, that $\alpha > 80^\circ$. At higher electron betas, the required tilt becomes smaller. Therefore, there is a chance that the modes predicted in this study can be observed at LAPD.

VII SIGNATURES OF THE INSTABILITY

In this section, we discuss characteristic signatures of the instability which may help to identify it in the experiments. The most obvious signature is the decrease of the amplitude of fluctuations with the distance from the absorbing plate. The higher beta, the faster is the decrease (provided of course that beta is higher than the critical value determined from the condition (22)).

The second prominent feature of the instability is its dependence on the mutual orientation of the tilt of the divertor plate and the temperature gradient. Assuming that the maximum of the electron temperature is situated at the separatrix, we predict that in a common flux region the short-wavelength instability is present for a “positive” tilt, and the long-wavelength instability is present at the “negative” tilt, whereas in the private flux region the situation is the opposite. This prediction can also be tested at the linear device by switching from the configuration of Fig. 4a to that of Fig. 4b.

The third feature is related to the direction and the magnitude of the phase velocity of oscillations. We note that, according to Eq. (17), the real part of the frequency is equal to

$$\text{Re}\omega = \text{Re}\Omega + \mathbf{k} \cdot \mathbf{v}_D \quad (67)$$

We discuss this relationship for the case of a substantial tilt considered in Sec. VI.B. In this case Eq. (37) yields the following expression for $\text{Re}\Omega$:

$$\text{Re}\Omega = -\frac{T_e' v_A \beta_e \frac{u}{v_i} \sqrt{\beta_e} (2\Lambda - 1) \left(1 + \frac{2B_T^2}{B^2 k^2 \rho_i^2} \frac{u}{v_i} \sqrt{\beta_e} \right) + \left(\frac{B}{B_p} \tan \alpha \right)^2 \sqrt{\beta_e}}{2T_e k_y \rho_i \left(k^2 \rho_i^2 + \frac{2B_T^2}{B^2} \frac{u}{v_i} \sqrt{\beta_e} \right)^2 + \beta_e k^2 \rho_i^2 \left(\frac{B}{B_p} \tan \alpha \right)^2} \quad (68)$$

Recalling Eqs. (4) and (5) defining the drift velocity, one can see that the term $\text{Re}\Omega$ universally corresponds to a contribution to phase velocity opposite to \mathbf{v}_D . One can check, however, that for the short-wavelength mode with $k\rho_i=1$, this contribution is small. In other words, the short-wavelength modes are advected with the $\mathbf{E}\times\mathbf{B}$ drift velocity. For the long-wavelength modes of a maximum growth rate (i.e., for the mode defined by conditions (52)), the contribution to the phase velocity coming from the term $\text{Re}\Omega$ in (67) is comparable to \mathbf{v}_D . Depending on the specific parameters of the system, the resulting phase velocity may become considerably smaller than \mathbf{v}_D or can even reverse sign.

The characteristic frequency of the perturbations, $f=\omega/2\pi$, is $\sim v_i/2\pi\Delta$ for the short-wavelength modes with $k\rho_i\sim 1$, and $v_i\beta_e^{1/4}/2\pi\Delta$ for the long-wavelength perturbations near the maximum of their growth rate. For the hydrogen plasma with $T_e=30$ eV, $\beta_e=3\cdot 10^{-4}$, and $\Delta=1$ cm, the frequency f of the short-wavelength mode is ~ 1 MHz, whereas the frequency of the long-wavelength mode is ~ 100 kHz. The characteristic wave number is $\sim (0.5-1)\rho_i^{-1}$ for the short-wavelength mode and $\sim (0.1-0.15)\rho_i^{-1}$ for the long-wavelength mode.

There is a correlation between the perturbation of the current density at the divertor plate and the temperature perturbation. Both quantities can be measured by flush-mounted probes. For the strong-enough tilt, one has, by the order of magnitude (see Eq. (33)):

$$\frac{\delta j_n}{enu} \sim \frac{\Omega \xi_x}{u} \sim \frac{\delta T_e}{T_e} \frac{\Omega \Delta}{u} \quad (69)$$

There is a subtlety here: strictly speaking, we cannot use expression (33) for the perturbation of the normal component of the current, because this expression pertains to the current at *the plasma side of the sheath*, whereas the flush-mounted probe measures the current at *the wall side of the sheath*; the two expressions are, generally speaking, different [20]. Using a convenient representations [22] for the two current densities (Eqs. (20) and (21) of Ref. 22), one sees that, to get the perturbation of the current at the wall side, one has to replace the factor $(\Lambda+0.5)$ by the factor $(\Lambda-0.5)$ in Eq. (33). This will not change an order-of-magnitude estimate (69).

It is also worthwhile to mention that, because of the tilt, the normal component of the unperturbed ion current density, $j_{n0}^{(i)}$, is much smaller than enu , namely $j_{n0}^{(i)} = enu(B_p/B)\cos\alpha$. If one uses $j_{n0}^{(i)}$ as a normalization factor, one gets, instead of (69):

$$\frac{\delta j_n}{j_{n0}^{(i)}} \sim \frac{\delta T_e}{T_e} \frac{\Omega \Delta}{u} \frac{B}{B_p \cos\alpha} \quad (71)$$

The magnetic field perturbation, although small, may be measurable. It can be evaluated from Eq. (19') which yields $\delta B \sim B(\Omega \xi_x / v_A)$. One can relate it to the temperature perturbation:

$$\frac{\delta B}{B} \sim \frac{\Omega \Delta}{v_A} \frac{\delta T_e}{T_e} \quad (72)$$

Vector of the magnetic field perturbation is perpendicular to unperturbed magnetic field.

VIII DISCUSSION

We have presented an analysis of an instability localized near the divertor plate. It is driven by an interplay between the sheath boundary conditions and bulk long-parallel wavelength Alfvén wave. The existence of the modes that would exponentially decay before reaching the X point requires finite plasma beta in the scrape-off layer and favors divertors with long divertor legs. The modes then become completely decoupled from any processes occurring near the X point and beyond it. The modes are present even in the absence of the curvature effects and have high growth-rates exceeding the inverse Alfvén transit time over the divertor leg. The instability increases in the presence of a significant “radial” tilt of the divertor plate.

We have identified two modes, the short-wavelength mode and the long-wavelength modes. One of them is unstable for the positive tilt, whereas the other is unstable at the negative tilt (the sign of the tilt is defined at the beginning of Sec. II). Therefore, if one of the modes is dominant in the common flux region, the other is dominant in the private flux region, and vice versa.

If the modes reach high-enough level, they may lead to a broadening of the scrape-off layer within the divertor leg, without having any direct effect on the plasma confinement in the SOL above the X point and, therefore, not causing any degradation in the confinement of the bulk plasma. This part of the problem needs, however, a nonlinear analysis which we leave for the future work. Also for the future work is left a more general study of the mode, where it would be only partly “detached” from the X point, so that one would have to deal with boundary conditions on both sides of the divertor leg.

The physics of these modes can be studied in linear devices, by using shaped end plates. It may be possible to detect them at the existing LAPD device.

Acknowledgments

The authors are grateful to Dr. G. D. Porter for helpful discussions of the plasma parameters in the divertors of fusion devices. This work was performed under the auspices of the U.S. Department of Energy by University of California Lawrence Livermore National Laboratory under contract W-7405-Eng-48.

Appendix 1.

Evaluating the maximum of the function $g(C, \tilde{k})$

To find $\mu \equiv \max_{\tilde{k}, C} g(C, \tilde{k})$, we solve equations $\partial g / \partial C = 0$, $\partial g / \partial \tilde{k} = 0$. These equations can be presented as:

$$C = \frac{1 + \tilde{k}^2}{\tilde{k}}; \quad \tilde{k}^4 + \tilde{k}^2(\Lambda + \frac{5}{2}) - (\Lambda - \frac{1}{2}) = 0$$

Solving these equations for \tilde{k} and C , one finds their values corresponding to the maximum of the function g :

$$C_{opt} = \frac{\sqrt{(\Lambda + 0.5)(\Lambda + 8.5)} - (\Lambda + 0.5)}{\sqrt{2}\sqrt{\sqrt{(\Lambda + 0.5)(\Lambda + 8.5)} - (\Lambda + 2.5)}}; \quad \tilde{k}_{opt}^2 = \frac{\sqrt{(\Lambda + 0.5)(\Lambda + 8.5)} - (\Lambda + 2.5)}{2}$$

The maximum value of the function g is

$$\mu \equiv \max_{\tilde{k}, C} g(\tilde{k}, C) = \frac{\left(3\Lambda + 1.5 - \sqrt{(\Lambda + 0.5)(\Lambda + 8.5)}\right)\sqrt{\sqrt{(\Lambda + 0.5)(\Lambda + 8.5)} - (\Lambda + 0.5)}}{2\sqrt{2}\left(\sqrt{(\Lambda + 0.5)(\Lambda + 8.5)} - (\Lambda + 0.5)\right)}$$

The plot of all these quantities vs. the parameter Λ is presented on Fig. 3.

Figure captions

Fig. 1. The geometry of the problem.

Fig. 2. The normalized growth rate. Parameters of the system are specified by Eq. (41). The numbers by the curves are the corresponding values of $\tan\alpha$. The plot corresponds to a positive tilt. One sees that short-wavelength modes become localized (in the sense of condition (22)) at $\tan\alpha > 4$. For the negative tilt, the picture turns “upside down,” and the long-wavelength mode becomes unstable. This mode is marginally localized for the set of parameters (41). It would be fully localized for somewhat longer divertor legs.

Fig. 3. Dependence of various parameters of the long-wavelength instability on the logarithmic factor Λ (see Appendix 1 for the derivation).

Fig. 4. The dependence of the dimensionless function h (Eq. (57)) on $k\rho_i$ for various values of β_e ; we assume that $\Lambda=2.5$, $u/v_{Te}=1.5$.

Fig. 5. The possible geometry of a linear experiment: a) the conical end surface corresponds to a positive tilt if the electron temperature decreases in the outward direction $T_e' < 0$; b) the conical surface corresponding to the negative tilt for the same sign of T_e' .

References

1. B.B. Kadomtsev, In: "Phenomena in Ionized Gases" (Proc. 7th Conf. Belgrade, 1965) Vol. 2, p. 610, Belgrade, 1966.
2. H.Berk, D. D. Ryutov, Yu. A.Tsidulko JETP Lett., **52**, 23 (1990).
3. H.Berk, D. D. Ryutov, Yu. A.Tsidulko. Phys.Fluids, **B3**, 1346 (1991).
4. H.L. Berk, R.H. Cohen, D.D. Ryutov, Y.A. Tsidulko, X.Q. Xu. Nuclear Fusion, **33**, 263 (1993).
5. D.Farina, R.Pozzoli, D. Ryutov. Plasma Phys. Contr. Fusion, **35**, 1271 (1993).
6. X.Q. Xu, R.H. Cohen R.H. Plasma Phys. Contr. Fusion, **35**, 1071 (1993).
7. K.Lotov, D. Ryutov, J. Weiland. Physica Scripta, **50**, 153 (1994).
8. D.R. McCarthy, P.J. Catto, S.I. Krasheninnikov. Phys. Plasmas, **8**, 750 (2001).
9. D.Farina, R.Pozzoli, D. Ryutov. Nuclear Fusion, **33**, 1315 (1993).
10. D.D. Ryutov, R.H. Cohen. , Contributions to Plasma Physics, **44**, 168 (2004).
11. J.R. Myra, D.A. D'Ippolito, X.Q. Xu, R.H. Cohen. Phys. Plasmas, **7**, 4622 (2000).
12. X.Q. Xu et al. Submitted to Nucl. Fusion.
13. Y.A. Tsidulko, H.L. Berk, R.H. Cohen. Physics of Plasmas. **1**, 1199 (1994)
14. W. Kunkel, J. Guillory. In: "Phenomena in Ionized Gases" (Proc. 7th Conf. Belgrade, 1965) Vol. 2, p. 702, Belgrade, 1966
15. A.V. Nedospasov. Sov. J. Plasma Phys., **15**, 659 (1989)
16. X. Garbet, L. Lauren, J.-P. Roubin, A. Samain. Nucl. Fusion. **31**, 967 (1991).
17. S.I. Krasheninnikov. Phys Lett.-A, **283**, 368 (2001).
18. W. Gekelman, M. Van Zeeland, S. Vincena, P. Pribyl P. Journal of Geophysical Research-Space Physics. **108**, 1281 (2003)
19. R. Chodura. Phys. Fluids, **25**, 1628 (1982).
20. R.H.Cohen, D.D. Ryutov. Phys. Plasmas, **2**, 2011 (1995).
21. D.Farina, R.Pozzoli, D.D. Ryutov. Phys.Fluids, **B5**, p.4055 (1993).
22. D.D. Ryutov. Contributions to Plasma Physics, **36**, 207 (1996).

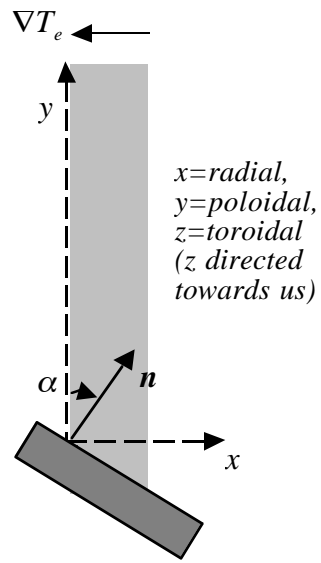


Fig. 1

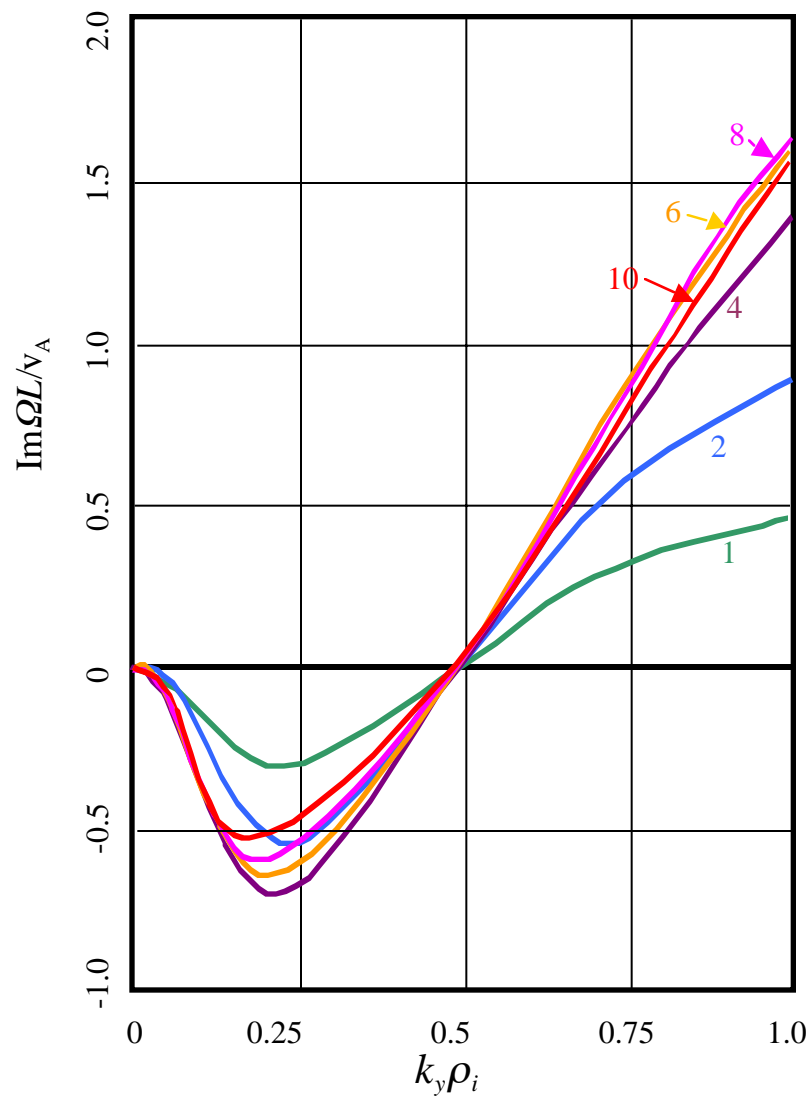


Fig. 2

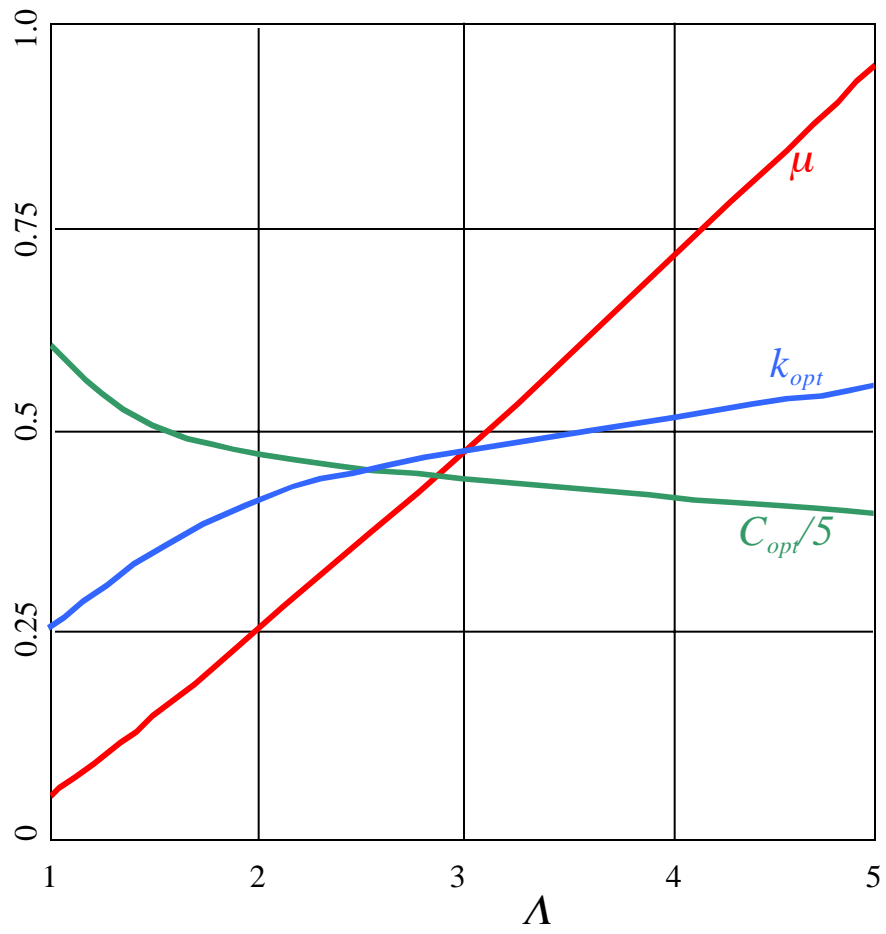


Fig. 3

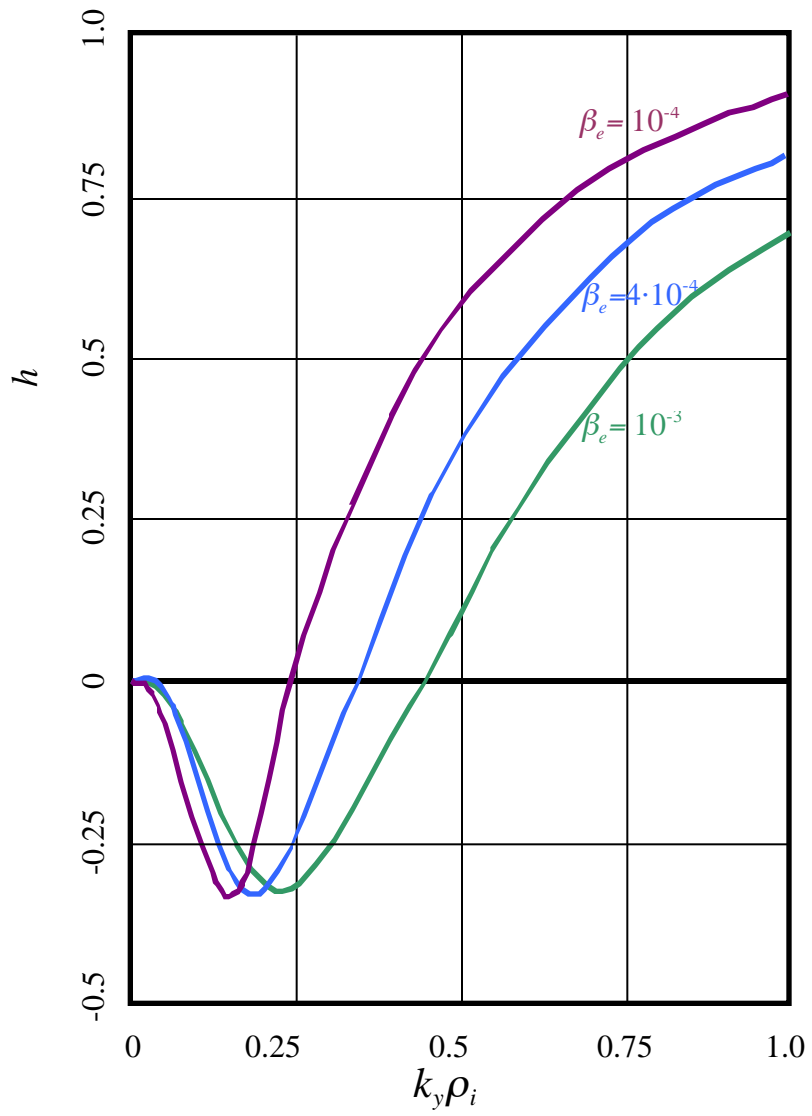


Fig. 4

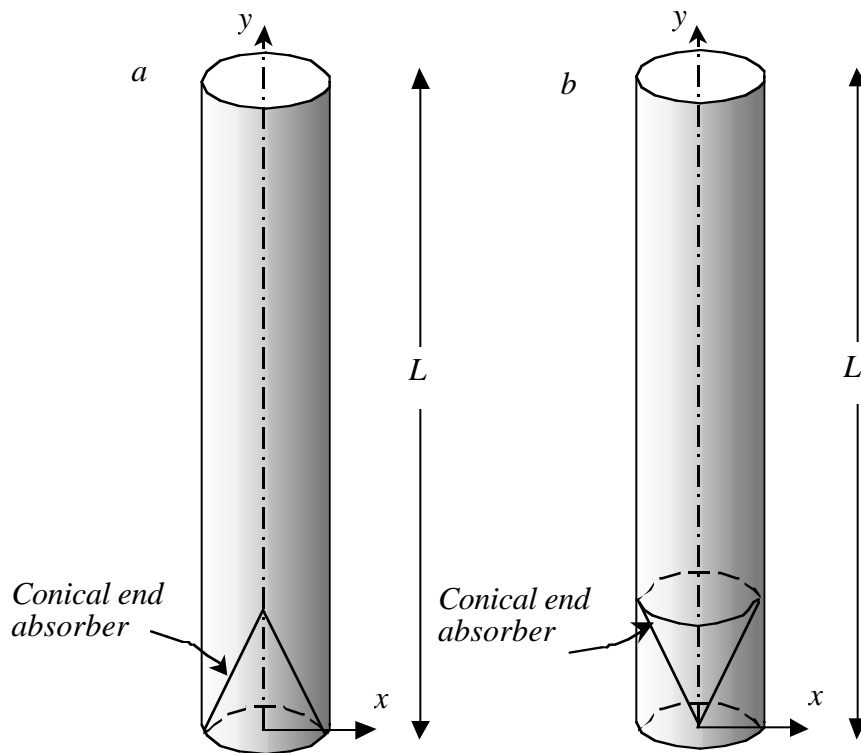


Fig. 5